UDC 621. 314. 63. 07

ELECTRIC FIELD AT THE SURFACE OF THYRISTORS

Kimitake Sumino
Central Research Laboratory
Kenjiro Umemura
Development Dept.

I. INTRODUCTION

The blocking voltages of power devices have increased rapidly over the last few years. High voltage device can be made by taking a serious view of the surface shape of the devices as well as improvements in manufacturing techniques such as surface treatment and diffusion. The surface shape is generally of the bevel structure which is used to insure the small surface field.

The main problem in raising the blocking voltages of semiconductor devices is generally conceded to be the problem of surface blocking voltages. The surface is very sensitive to the atmosphere and the electric field in the surface is influenced by surrounding gases, moisture, protective films, etc. When the surface field becomes greater in certain places, the current often flows concentrically in such places,[1] and the blocking voltage decreases. Therefore, in order to keep the blocking voltage high, the field distribution must be uniform and high value in one place must be avoided. The surface field also varies in accordance with the surface conditions and the blocking voltage has been raised by measures of improvements of etching and protective varnish. However, the great improvements in the blocking voltage recently have been due mainly to the bevel construction which provides angular shapes oblique in respect to the junction surface. R. Davies[2] has reported on the theoretical aspects of field distribution when the bevel structure is used, and that of the high voltage diode has already been introduced.[3]

Since there are two blocking junctions in a thyristor, the double bevel construction in which two bevel angles are combined is adopted. This structure is arranged in such a way that decreases the surface field under the forward and reverse biases, but generally, the forward blocking voltage includes more problems.

In this article, several cases of the surface field distribution of a thyristor in forward bias will be introduced. It is shown that if appropriate conditions are selected for the double bevel construction, the surface field can be reduced and this is highly effective in improving the blocking voltage and stability.

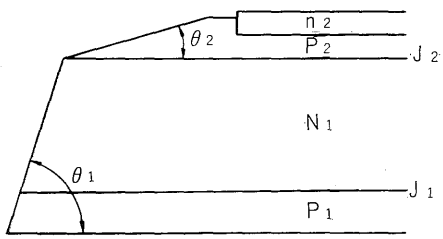

Fig. 1 Double bevel structure of thyristor

II. DETERMINATION OF SURFACE FIELD DISTRIBUTION

As was mentioned above, only the surface field distribution for forward bias was investigated for this article. The double bevel structure of thyristor has two bevel angles on the junction surface as is shown in *Fig. 1*. The angle θ_1, in the figure is comparatively large while θ_2 is small. With this structure, the surface fields in respect to the forward and the reverse bias can be kept lower and the blocking voltage can be improved. The surface field distribution in forward bias is considered to be the distribution of the part formed by the angle θ_2 when the junction J_2 is under reverse bias.

The surface field distributions are determined experimentally by the probe method and theoretically by a method based on that of R. Davies[2] in which the surface potential distribution is calculated and the surface field distribution is determined from the slope of the potential curve. An outline of the method to determine the potential distribution will be given below.

1. Exprimental Method

Fig. 2 shows the measuring apparatus and *Fig. 3* is an outline of the measuring method. The measuring apparatus consists of a probe for measuring the potential, a sample stage and a micromanipulator for moving the sample.

For the measurement, a suitable voltage is applied in the forward direction between the anode and the cathode of the sample thyristor, the probe is placed on the P_2 layer surface of the cathode side; the voltage is measured between the anode and the probe

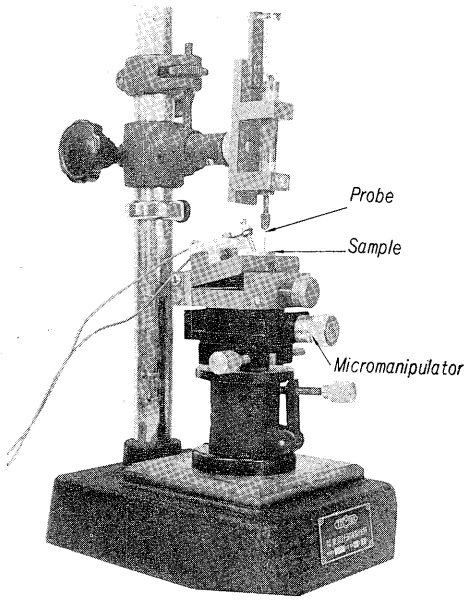

Fig. 2 Measuring apparatus

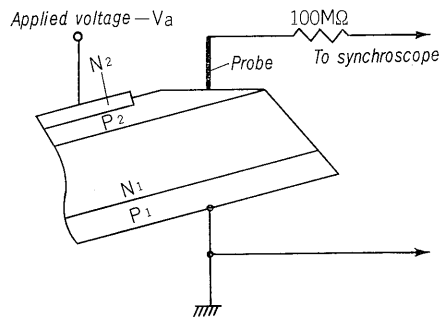

Fig. 3 Measuring method

with a synchroscope. If the sample is moved at regular intervals by the micromanipulator and the measurement is repeated each time, a potential curve for the surface can be obtained and the surface field distribution can be determined.

2. Theoretical Method

This method is exactly the same as that used in the case of the diode[3] and is based on the work of R. Davies.[2] Since the sample is of a disk, it is sufficient to determine the field distribution in the plane which passes through the center of the disk. It is necessary to decide on a suitable size for this plane so that the size does not influence the field distribution of the part to be calculated.

The first step in the calculation is to construct nodes by dividing the plane at regular intervals in horizontal and vertical direction respectively. It is very easy to carry out the calculation if the nodes are arranged so that they conform exactly to the junction surface for which the field distribution is to be determined. *Fig. 4* shows the potential $U_0(x_0, y_0)$ at the point (x_0, y_0) and the potentials U_T, U_B, U_L and U_R of the four nearest neighbor nodes, and the

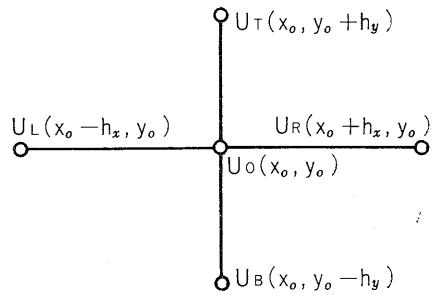

Fig. 4 Node

subscript T, B, L and R represents top, bottom, left and right respectively. For the calculation, first the initial potential values at the nodes are determined approximately and these values are corrected by means of calculations. The potential $U_0(x_0, y_0)$ is related to the potential U_T, U_B, U_L and U_R at the nearest neighbor nodes and the electric charge N_0 (x_0, y_0) at the point (x_0, y_0) as shown in equation (1). With this equation, a new approximate value of U_0 can be obtained.

If this calculation is repeated for other nodes, this approximation can be improved.

$$U_0=\frac{1}{2\left(\frac{1}{h_x^2}+\frac{1}{h_y^2}\right)}\left\{\frac{U_L+U_R}{h_x^2}+\frac{U_T+U_B}{h_y^2}+\frac{qN_0(x_0, y_0)}{\varepsilon_0\kappa_0(x_0, y_0)}\right\} \quad \cdots\cdots\cdots\cdots(1)$$

These calculations are continued until the potential variation at the nodes becomes less than some prescribed value. If the potential distribution in the plane is determined in this way, it is possible to obtain the field distribution on the surface.

III. RESULTS OF EXPERIMENTS AND CALCULATIONS

The surface field distribution in forward bias of the thyristor was obtained by using the above-mentioned experimental and theoretical methods. In thyristor with the double bevel structure, various parameters such as the bevel angle, the impurity concentration profile and the width of P_2 layer were varied and the surface field distribution was determined for each case. It was evident from the results that the surface field distribution can be decreased by selecting

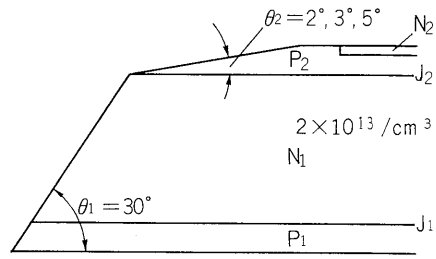

Fig. 5 Sample

the most appropriate values of such parameters. This proves that the double bevel structure is sufficiently effective in respect to high blocking voltages.

The structure of the samples used for the experiment and the calculation is shown in *Fig. 5*. The anode side bevel angle θ_1 was kept constant at 30° and the smaller angle θ_2 was varied. The bevel angle changes from θ_1 to θ_2 on the surface of the J_2 junction.

1. Bevel Angle θ_2 and Surface Field Distribution

Fig. 6 shows the calculated results of the surface field distribution for bevel angles of 2°, 3° and 5. In it, the single diffusion profile is the usual impurity concentration profile and the double diffusion profile is a combined one of two ordinary profiles. The impurity concentration profiles for each case are shown in *Fig. 9*. The single diffusion profile is shown as Ⓐ and the double diffusion profile as Ⓐ+Ⓑ. *Fig. 7* shows the relationship between the peak electric field and the bevel angle for double diffusion profile.

From these results, it is evident that the smaller the bevel angle, the smaller the surface field, and a smaller θ_2 is also better in terms of blocking voltage. Beveling the surface at very small angle is very difficult but it is possible to achieve an angle of 2°.

2. Impurity concentration Profile of P_2 Layer and Surface Field Distribution

The results for the impurity concentration profile of P_2 layer are clearly shown in *Fig. 6*. *Fig. 8* shows the calculated values of surface field distribution when the higher concentration part Ⓐ of double diffusion profile as shown in *Fig. 9* was held constant and the lower parts Ⓑ, Ⓒ and Ⓓ were changed. Impurity profiles Ⓐ, Ⓑ, Ⓒ and Ⓓ shown in *Fig. 9* are complementary error functions. In these examples, the lower the surface impurity concentration C_0, the lower the surface field strength. The lowest value was found for the profile Ⓓ.

In the forward bias, the greatest amount of voltage

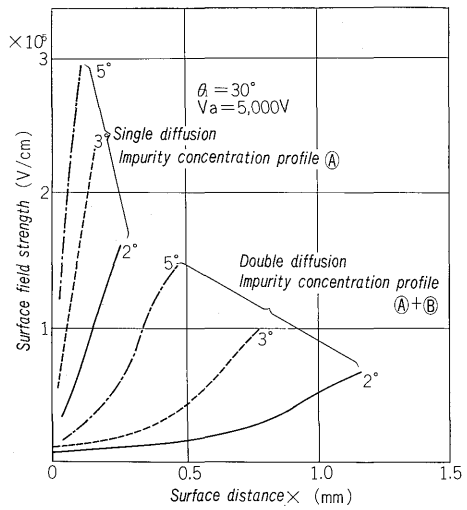

Fig. 6 Relationship between surface field distributions and impurity concentration profiles, bevel angles

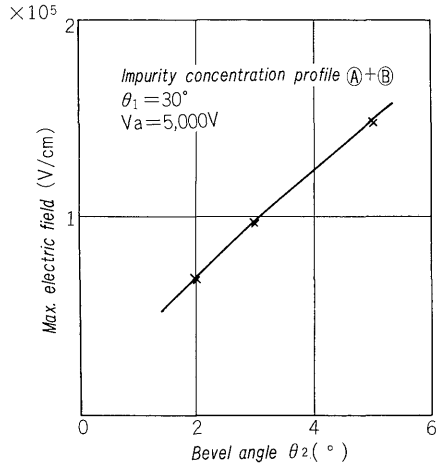

Fig. 7 Relationship between peak electric field and bevel angle θ_2

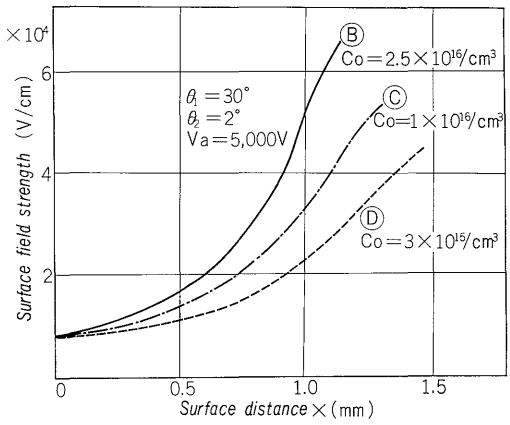

Fig. 8 Relationship between surface field distributions and impurity concentration profiles (1)

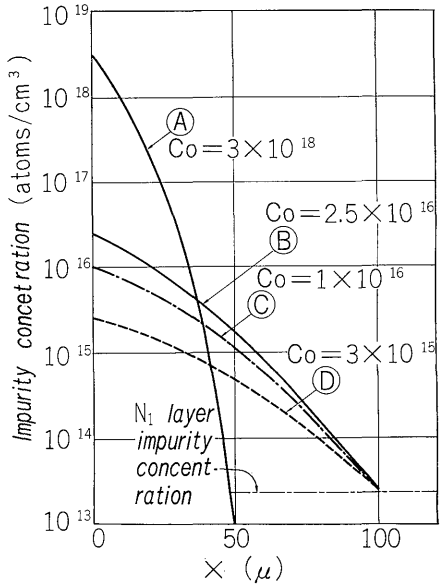

Fig. 9 Impurity concentration profiles (1)

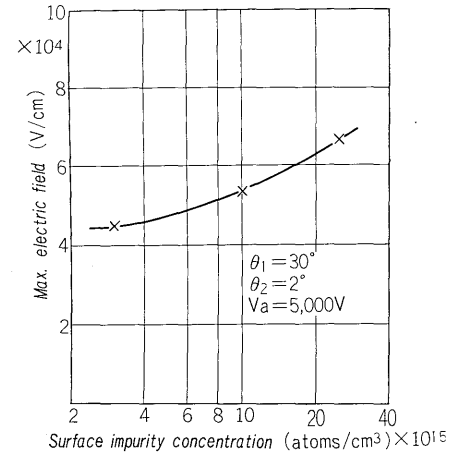

Fig. 10 Relationship between peak electric field and impurity concentration profiles

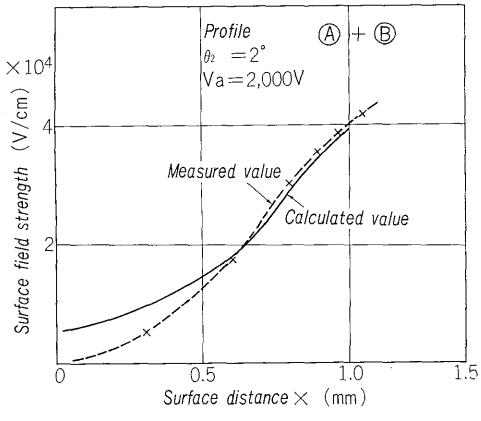

Fig. 11 Comparison between measured and calculated values of surface field

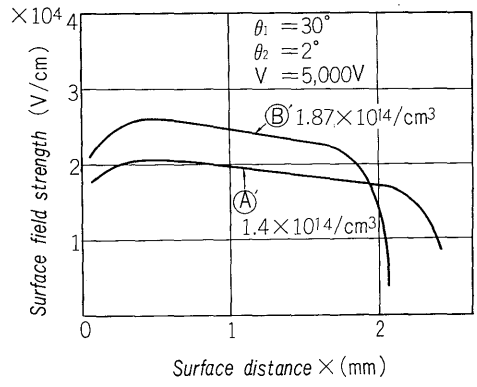

Fig. 12 Relationship between surface field distiributions and impurity concentration profiles (2)

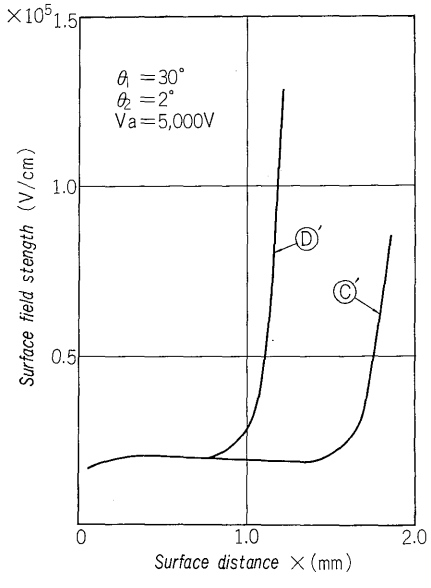

Fig. 13 Relationship between surface field distributions and impurity concentration profiels (3)

is applied to the P_2 layer in the surface and the depletion layer width of the P_2 layer near the surface is almost equal to the inside depletion layer width.

Thus when the impurity concentration in P_2 layer near the N_1 layer is lower, the overall surface field will become lower since the depletion layer of P_2 layer expanded widely. The peak surface field will also occur in the high concentration side of the P_2 layer. *Fig. 10* shows the relation between this peak and the impurity concentration profiles used in the examples shown in *Fig. 8*.

From these results, it can be seen that surface field distribution varies with the impurity concentration profile, and the field can be kept lower if the profile is carefully controlled. *Fig. 11* shows a comparison of these calculated results with the experimental results. There was good agreement even when the applied voltage was 2,000 V.

3. Uniform Impurity Concentration

In the examples given so far, it has been shown that the surface field strength can be decreased, if the P_2 layer impurity concentration near the N_1 layer is low and the depletion layer is expanded. The expansion of the depletion layer is limited at high impurity concentration part in P_2 layer and there the peak field appeares.

The following are the cases for a uniform impurity concentration profile of P_2 layer, which can be achieved by using such methods as epitaxial growth. These results are shown in *Fig. 12* and *13* and the impurity concentration profiles for each case are shown in *Fig. 14*.

In these cases the P_2 layer is divided into two parts, P_{21} and P_{22}. The impurity concentration of P_{21} layer is kept lower in order to expand the depletion layer widely. The P_{22} layer with higher impurity concentration suppresses the current amplification factor α_{npn} so that the static forward blocking capability and the dynamic dv/dt capability are not decreased. *Fig. 12* shows the case when the width of P_{21} is 100 μ and the impurity concentration in P_{21} is varied. In these cases the depletion layer does

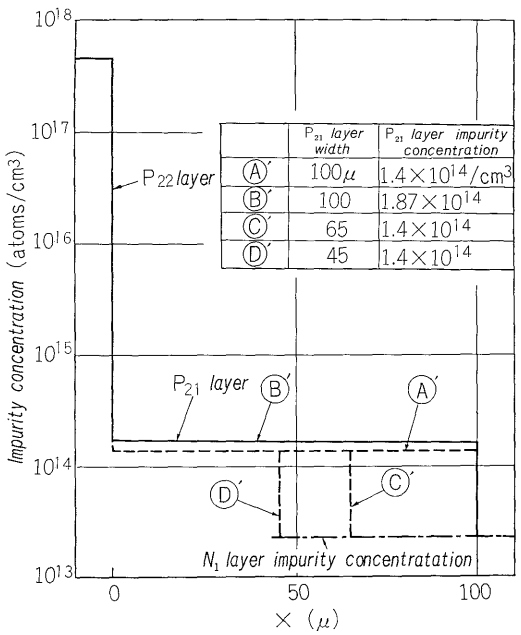

Fig. 14 Impurity concentration profiles (2)

not reach the P_{22} region. In such a case, the surface field becomes lower when the impurity concentration can be kept lower and the depletion layer wider. This tendency is the same as the tendency for double diffusion profile as shown in *Fig. 8*. However, unlike in the previous results, there is no field peak and the field is distributed uniformly. When $N_{p21}=1.4\times10^{14}/\text{cm}^3$, the maximum surface field with an applied voltage of 5,000 V is 2.1×10^4 V, which is a sufficiently low value. Considering the impurity concentration profile, the surface field can be decreased with the double bevel structure even with high applied voltages and it is possible to increase the blocking voltage sufficiently.

Fig. 13, shows the examples in which the depletion layer expands to cover whole P_{21} layer and reaches the P_{22} layer and the peak field appears in the P_{21} and P_{22} boundry region. These were also seen in the case of the punch-through type diode,[3] i.e. when the depletion layer expands to the P_{22} layer at a lower voltage, the peak value increases.

To make the surface field small, the bevel angle θ_2 must be small, impurity concentrations of P_2 layer which dicide the depletion layer width must be low and it's width must be such that even the depletion layer on the surface does not reach the P_{22} region. However, since the forward conducting characteristics are also influenced by the width of the P_2 layer,[4] it can not be made too wide. In the actual design, the blocking voltage and the forward conducting characteristics both have to be considered and the most suitable values of the concentration and the width of P_2 layer must be selected. In this way, it is possible to achieve a sufficiently low value of the surface field with a uniform impurity concentration profile without sacrificing the forward conducting characteristics.

IV. CONCULSION

This article has presented an outline of the surface field distribution in the forward biased thyristors under several different conditions. With sufficient designing using the double bevel structure, the surface field can be decreased and the blocking voltage can be raised sufficiently without sacrificing other characteristics such as the forward conducting characteristics.

Appendix

When calculating the surface field, equation (1) used. However, equation (2) as follows is used when the boundry of the inner and outer part of Si is between the point (x_0, y_0) and the neighboring node points.

$$\frac{U_L}{h_x^2\left\{\frac{\kappa_0}{\kappa_1}(1-\xi_L)+\xi_L\right\}}+\frac{U_R}{h_x^2\left\{\frac{\kappa_0}{\kappa_1}(1-\xi_R)+\xi_R\right\}}+\frac{U_T}{h_y^2\left\{\frac{\kappa_0}{\kappa_1}(1-\eta_T)+\eta_T\right\}}+\frac{U_B}{h_y^2\left\{\frac{\kappa_0}{\kappa_1}(1-\eta_B)+\eta_B\right\}}-U_0\left[\frac{1}{h_x^2\left\{\frac{\kappa_0}{\kappa_1}(1-\xi_L)+\xi_L\right\}}+\frac{1}{h_x^2\left\{\frac{\kappa_0}{\kappa_1}(1-\xi_R)+\xi_R\right\}}+\frac{1}{h_y^2\left\{\frac{\kappa_0}{\kappa_1}(1-\eta_T)+\eta_T\right\}}+\frac{1}{h_y^2\left\{\frac{\kappa_0}{\kappa_1}(1-\eta_B)+\eta_B\right\}}\right]+\frac{qN(x_0,y_0)}{\varepsilon_0\kappa_0(x_0,y_0)}=0 \quad \cdots\cdots\cdots\cdots(2)$$

In this equation κ_0, κ_1, ξ_L, ξ_R, η_T and η_B are according to Davies.[2]

References :

(1) C.G.B. Garrett, W.H. Brattin: J.A.P. 27 299 (1956)
(2) R. Davies, F. Gentry: IEEE Trans on Electron Devices ED-8 313 (1964)
(3) Sumino and Umemura: Surface Field Distribution of High Voltage Silicon Devices, Fuji Electric Journal, 42, No. 2 (1969)
(4) Haruki, Yokoyama: Current Voltage Characteristics of Thyristor, Fuji Electric Journal, 40, No. 9 (1967)